Hydrogen Bonding in 1,1′-Bi-2-naphthol within the Polarizable Continuum Model

Nikola Biliškov and Goran Baranović*

Division of Organic Chemistry and Biochemistry, Rudjer Bošković Institute, Bijenička c. 54, HR-10002 Zagreb, Croatia

Received: March 03, 2008; Revised Manuscript Received: July 05, 2008

Intra- and intermolecular hydrogen bonding of 1,1′-bi-2-naphthol in a series of solvents and in solid phase has been investigated by means of mid-IR spectroscopy and DFT reaction field calculations. The polarizable continuum model has been used to estimate the relative stability of isomers differing in the positions of the hydroxyl groups. The height of the potential barriers between them was also calculated and the corresponding transition states characterized. In hydrogen bond nonaccepting solvents, the isomer preference does not change relative to the gas phase, although the less stable isomers are more probable in solvents of higher relative permittivity. In hydrogen bond forming solvents, the least stable isomer is most probably prevalent due to the additional stabilization through intermolecular hydrogen bonds with solvent molecules. A detailed vibrational analysis revealed the spectral regions specific to the OH vibrations with the observed solvent effects concerning the redistribution of vibrational intensities rather than wavenumber shifts.

1. Introduction

Two atropisomeric forms of the 1,1′-bi-2-naphthol (BINOL) molecule are among the most widely used ligands in asymmetric synthesis.[1] The interactions between the two hydrogens at positions 8 and 8′ and between the two hydroxyl groups in *ortho*-positions to the covalent single C−C′ bond connecting the two naphthyl groups prevent free rotation around this bond. (Figure 1). The racemization is greatly facilitated in acidic or basic conditions and is considered almost impossible under neutral conditions and at room temperature. Deprotonation of the hydroxyl groups in very basic solutions results in the formation of $BINOL^{2-}$ anions that relatively easily undergo enantiomeric change. Within the computational study of racemization pathways of the BINOL molecule,[2,3] the internal rotation around the central C1C1′ bond was taken as the main reaction coordinate, and the transition states were located by the intrinsic reaction coordinate (IRC) method. As the dihedral angle between the two naphthyl groups had to pass through either 0° or 180°, rather high potential energy barriers, i.e., large deformations of molecular structure were implied. The racemization pathways under neutral conditions are energetically much less demanding if the hydroxyl rotations around the CO bonds are also included. In other words, for chiral molecules such as BINOL with relatively weak intramolecular hydrogen bonds (H-bonds) to π-electrons the enantiomeric change is intimately connected to the conformational equilibrium in solution wherein molecules alternate between being intra- and/or intermolecular hydrogen bonded.

Although the racemization does not take place at room temperature and under neutral conditions, there might still be three energetically feasible stable isomers of the BINOL molecule complicating its vibrational dynamics in solution. They are defined with respect to the positions of the hydroxyl groups (coplanar in each case with the naphthyl moieties): (a) both hydroxyl groups are directed away from the neighboring naphthyl moiety (*tt*-isomer), (b) one points away, and another is in interaction with the neighboring naphthyl π-system (*ct*-isomer), and (c) both hydroxyl groups are oriented toward the naphthyl π-systems (*cc*-isomer). In their ground electronic state, *cc*- and *tt*- molecules have C_2 symmetry. A BINOL molecule can be considered as made of two 2-naphthol molecules. There are two isomers of 2-naphthol, one with the OH group toward the long molecular axis (*trans*), and the other away from the axis (*cis*). The former builds the *tt*-isomer, while the latter is used for the *cc*-isomer. Such a conformational change is thus described by the two torsional angles, ∠(C1,C2,O,H) and ∠(C1′,C2′,O′,H′), around the CO bonds. All three types of BINOL isomers can be found in the solid phase, *cc* isomers in the crystal of racemic BINOL,[4] *ct* in inclusion compound of BINOL-acetone, and *tt* isomers in BINOL-dimethyl sulfoxide (DMSO),[5] BINOL-tetrahydrofuran (THF),[5] and in BINOL-*N*,*N*′-dimethylformamide (DMF).[6]

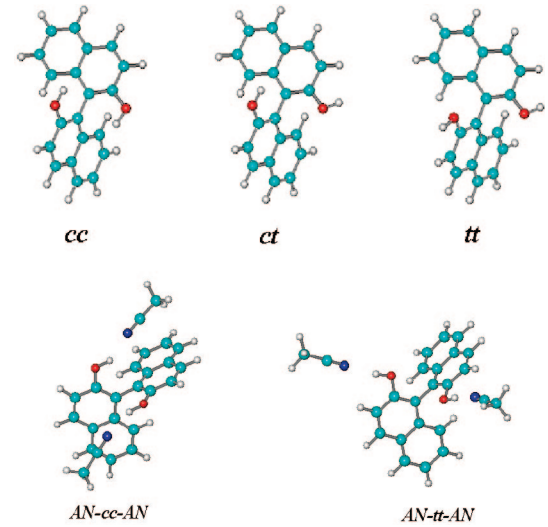

Figure 1. Three isomers of 1,1′-bi-2-naphthol defined by the positions of the OH groups and two hydrogen bonded complexes of BINOL with acetonitrile.

BINOL has been the subject of spectroscopic work mainly in connection with its chirality. It has been shown that the

* Corresponding author. Phone: +385-1-468-0116. Fax: +385-1-468-0195. E-mail: baranovi@irb.hr.

10.1021/jp801868x CCC: $40.75
Published on Web 08/06/2008

vibrational circular dichroism (VCD) spectra of the OH-stretching vibrations remarkably change with the solvent ability to accept hydrogen bonding with BINOL.[7] The VCD spectra of BINOL in the mid-IR region[8] covered the region 1700−1200 cm^{-1}. Since all the spectra were recorded in DMSO ($\varepsilon = 46.7$), most probably only BINOL molecules hydrogen bonded to solvent molecules were observed. The studied spectral region contains in its lower half the bending vibrations of the OH groups. However, the lowest analyzed band was at 1344 cm^{-1}, meaning that all the analyzed bands were actually due to the vibrations of the binaphthyl core (they therefore occur in closely lying doublets). Presumably, the vibrational spectrum of only the highest-energy *tt*-isomer was calculated in vacuo at the BPW91/6−31G(d,p) level of theory. The calculated vibrational spectrum revealed no modes in the measured range, which could be characterized as more or less pure in-plane O−H bending vibration. In addition to that, the lowest-lying CO torsion was claimed to be mixed with much higher stretchings and in-plane bendings of the aromatic cores. Two Raman studies have also appeared, dealing with neutral BINOL and its dianion formed by deprotonation of the hydroxyl groups in basic solutions.[9,10] In the solid phase, BINOL molecules are hydrogen-bonded between themselves, while, for example, in acetone solution ($\varepsilon = 20.70$) they are bonded to the solvent molecules. This has not been explicitly considered, and in analyzing the recorded vibrational Raman spectra, the calculated spectra (at the B3LYP/6−31G(d) level) of only the most stable *cc*-isomer were used. On the basis of visual inspection of the calculated Cartesian normal mode displacements, it was claimed that the CO stretchings were involved in the normal modes around 1600 cm^{-1}.[10] Thus, in some points the vibrational spectra of BINOL were interpreted in an unusual way, and we have decided to undertake a detailed vibrational study of BINOL in its ground electronic state describing the normal modes in terms of internal coordinates.

In the gas phase or in a solvent such as CCl_4 (often regarded as inert, but due to the electron accepting property of its chlorine atoms, it is not), BINOL and similar systems (alcohols) are characterized by two IR bands in the region 3700−3300 cm^{-1} (similar molecules with π-electrons belonging to an aromatic moiety such as 2-phenyl-phenol, 2,2′-dihydroxy-biphenyl, etc. have been also studied long ago[11−14] (along with other cases of intramolecular H-bonds to π-electrons of double or triple bond[13,15−17] that will not be treated here). The one at higher wavenumbers is assumed to be due to the free OH groups, while the second one is then due to the intramolecular H-bond (it is usually broader). The fact that BINOL in the gas phase weakly absorbs at 3648 cm^{-1} and strongly at 3562 cm^{-1} while 2-naphthol absorbs only at 3654 cm^{-1}[18] indicates a weak intramolecular O−H···π H-bond in BINOL. Therefore, an equilibrium between the isomers differing only in the positions of the OH groups is implied even in the gas phase. On the basis of temperature dependent IR spectra, the values for the enthalpy difference between the isomers, ΔH, within 0.5−2.0 kcal/mol were deduced for *ortho*-trityl phenols[19] and *ortho*-substituted phenols.[14,16] Since in these systems the OH groups stay predominantly in the hydrogen bonding range of the aromatic π-clouds, the internal rotation around the CO bond is expected to be highly hindered. In other words, the energetically unfavorable isomers should be barely present even in media of high dielectric strength. How high are the barriers for the hydroxyl group rotation in solvated BINOL? We shall find out in this study from the reaction field calculations and compare them with the available literature data on similar systems.

It is well known that phenols readily form hydrogen bonds with ketones and amides, which has also been established by IR studies of these systems most often in CCl_4. Thus, by using mixtures of solvents, a study of the isomerization equilibrium as a function of solvent properties would be possible. However, the present study has been envisaged as a prerequisite for getting equilibrium constants and enthalpies of BINOL complex formation. From only mid-IR measurements, it would be almost impossible to establish the true nature of the complex because an additional complication comes from the fact that even *cc* isomers can act as proton donors. In a binary system, the conformational equlibrium can be shifted,[20] and this is expected to happen when BINOL is dissolved in a neat solvent and depending on the H-bond acceptance ability of the solvent. This ability is quantified as parameter β within the Kamlet−Taft linear free energy relationships.[21] The present work will be concentrated on the interactions of BINOL with a series of solvents divided into two groups according to their β-values that are obviously important when BINOL is proton donating (a) non-hydrogen bonding solvents (non-H-bonding) such as carbon tetrachloride, CCl_4, chloroform, $CHCl_3$ (usually performs as non-H-bonding solvent, although it could be a proton donor when interacting even with strong H-bond π-acceptor), and dichloromethane, CH_2Cl_2 (for all of them $\beta = 0.10$[22]), and (b) H-bonding solvents such as DMF (a model of amide sites, $\beta = 0.69$), THF, $\beta = 0.55$, and acetonitrile (AN), $\beta = 0.40$. Acetone, $\beta = 0.43$, and DMSO, $\beta = 0.76$, which were also used in the previous studies[8,10] are strong H-bond acceptors. Within the polarizable continuum model (PCM),[23] the solvent permittivity ε is an essential parameter ($\varepsilon(CCl_4) = 2.228$, $\varepsilon(CHCl_3) = 4.9$, $\varepsilon(CH_2Cl_2) = 8.93$, ε(THF) = 7.58, ε(AN) = 36.64, and ε(DMF) = 36.7). Obviously, the β-scale closely follows that of ε, and subsequently it will be enough in the discussion below to use only permittivity.

We will be thus dealing with some other properties of solvated BINOL such as the positions of the most sensitive vibrations with respect to the conformational changes related to the orientation of hydroxyl groups, the wavenumber shifts induced by the nonspecific part of the solute−solvent interactions, and the influence of the nonspecific solute−solvent interactions on the free energy differences and barrier heights separating three isomers, and also on the nature of the transition states between them. Strictly speaking, the results from PCM calculations are to be related only to non-H-bonding solvents. For any of the H-bonding solvents, an intermolecularly H-bonded BINOL with at least one or two solvent molecules embedded in the polarizable continuum should be taken into consideration. In order to get a more complete picture of the H-bonding in BINOL, preliminary results along these lines will also be presented here. Three ε-values, those of CCl_4 (low), CH_2Cl_2 (medium), and AN (high), were chosen in the reaction field calculations to obtain the optimized geometries and harmonic vibrational frequencies of three solvated BINOL isomers. The infrared intensities of the BINOL νOH···π band and some other naphthyl deformation bands have also been calculated[24] and compared with experimental values, not only qualitatively but also quantitatively in the selected non-H-bonding solvents.

2. Materials and Methods

2.1. Experimental Procedures. BINOL (99%) was purchased from Aldrich and used without further purification. It is poorly soluble in most nonpolar solvents (only CCl_4 was used). As polar solvents, dichloromethane, chloroform, AN, DMF, and THF were used. Solvents were purified before use (an antioxi-

dant is normally found in chloroform and THF) by the standard methods.[25] Solutions were made up using Hamilton microsyringes immediately before spectral acquisition. The concentrations of BINOL were between 0.002 and 0.2 mol dm^{-3}. Infrared spectra were collected using an ABB Bomem MB102 spectrometer, equipped with CsI optics and a DTGS detector. Spectra were acquired and treated by Grams/32 software, version 5.2, with a spectral resolution of 1, 2, or 4 cm^{-1} in demountable liquid cells (KBr, CaF_2, or silicon). The measurements were carried out at room temperature of (21 ± 2) °C. The cell path length nominally was in the range from 200 to 5000 μm. All of the pathlengths were measured interferometrically or by using the secondary standard method as developed by Bertie et al.[26] The recorded spectra were also analyzed by means of SpekWin32 software.[27] In order to enable correct comparison with similar systems, the IR spectra of 2-naphthol (Aldrich) (as solid and in solutions) and phenol (Aldrich) were also recorded.

2.2. Calculations. The calculations were performed with the Gaussian 03 suite of programs[28] at the B3LYP/6−31+G(d) level, i.e., with a hybrid functional B3LYP combined from Becke's three-parameter exchange functional[29] and Lee, Yang, and Parr's correlation functional[30] with the standard basis set 6−31+G(d).[31] The choice of both the functional and the basis set is important. The B3LYP functional has shown good performance in predicting various molecular properties,[32] while the chosen basis set should be satisfactory because vibrational frequencies and free energies of solvation and not covalent bond dissociation enthalpies are considered here. Since none of the BINOL conformers is built from two loosely bound parts, the molecular energies are not expected to be significantly affected by the basis set superposition error (BSSE). However, it had to be taken care of when H-bonded clusters of BINOL with solvent molecules were calculated. The vibrational frequencies of free molecules were scaled by a factor of 0.9648. This value is based on the empirical assignment of the gas phase phenol spectrum[33] (transferability of the scale factor is thus assumed) and has been determined as the best value in the least-squares sense. In favor of the assumed transferability, it is worth mentioning that it is quite close to 0.963, which was obtained for the B3LYP/6−31G(d) (no diffuse functions) frequencies of diphenyldiacetylene (pure hydrocarbon molecule) also from the corresponding empirical assignment.[34] A relative error of 1% above ∼500 cm^{-1} and up to 9% below ∼500 cm^{-1} might be expected after scaling the calculated wavenumbers. The scaling is justifyingly performed only if the calculated frequencies of a free molecule are to be compared with the low-resolution gas phase data. When a solvated molecule is calculated in any of the reaction field models whereby wavenumbers are downhifted due to the solute−solvent interactions, the uniform scaling by the same scaling factor is of doubtful meaning. Nevertheless, it will be used here so that the calculated solvent induced wavenumber shifts will also be scaled.

The solute−solvent interaction was evaluated using the reaction field theory of polarizable continuum.[23] The shape and size of a solute molecule is defined by placing the solute in a cavity built by putting a sphere of a certain radius around each solute atom on which a solvent sphere of predefined radius is rolled (solvent excluding surface). We used Bondi's atomic radii.[35] The inclusion of hydrogen radii was considered essential because the BINOL isomers are distinguished by the position of the hydroxyl hydrogens. Except for the dielectric constant value and in some cases the average area of the tesserae, all other internal parameters defining the solvent had the default values. The convergence of geometry optimization of a solvated molecule was sometimes very difficult to achieve (especially for the higher values of ε) which forced us to vary the size of the tesserae (not only TSARE = 0.2 (the default value), but 0.1 and 0.3 were also tried). The CPU time and the memory used during calculations strongly depends on it. It is, however, more important that the differences in the calculated wavenumbers and IR intensities can be up to 3−4% at either direction of the TSARE = 0.2 results. Thus, the size of tesserae might be of some relevance for the CPU times but cannot be expected to improve the agreement with the experiment. Similar considerations apply for the factor ALPHA, which can be used to multiply Bondi's radii but only if using the option of user defined spheres. Since it is expected that the limit of a vibrational frequency for a large enough cavity should be the gas phase value, the size of the solute cavity certainly influences the calculated values not only of frequencies but also of energies as well. By choosing different values of ALPHA, one might hope to avoid the enormous convergence problems occurring when trying to get the optimized geometry, in particular of a transition state, in a solvent of high permittivity. However, this is not possible because the chosen value of ALPHA different from 1.0 is used only in the first optimization step.[36] These are important details when the performances of the model are tested against an experimentally well characterized system. However, any improvements along these lines cannot surpass the basic deficiency of the model of not taking into account any specific solvent−solute interaction such as H-bonding, which certainly plays a decisive role in BINOL conformational equilibrium in H-bond forming solvents.

3. Results and Discussion

3.1. Calculated Structures and Conformational Isomerism in the Gas Phase. Even the selected H-bond structural parameters (Table 1) of the three isomers in vacuo or in solution are not much different. Practically no changes from gas to solution or among different isomers of other geometry parameters are predicted. It is generally assumed that the formation of an H-bond is accompanied by shortening of the O−H bond, but here, an elongation by 0.005 Å is calculated instead. The dihedral angle C(CC′)C′ is smaller by only 3° in isomers without intramolecular H-bonding. This is rather different from what has been obtained at slightly different levels of calculations, B3LYP/6−31G(d),[2] where the values of 97°, 87°, and 88° were reported for *cc*, *ct*, and *tt* isomer, respectively. Although arbitrarly chosen, the distance (O)H···A (Table 1) being in the interval 2.33−2.40 may be considered typical for this type of H-bond. The fact that the gas phase or PCM values do not follow the trends observed for the crystal structures of the racemic or optically pure BINOL and its inclusion compounds is due to the intermolecular forces. The dihedral angle C(CC′)C′ is strongly affected by the way the molecules are packed in the crystal. The packing pattern is greatly determined by the intermolecular H-bonds, and therefore, the OH bond lengths of the two hydroxyl groups cannot be the same.

Thermodynamic data on the relative stabilitiy of three BINOL isomers in the gas phase (Table 2) are in favor of the predominance of the *cc*-isomer. The Gibbs energy differences for free isomers are not enormous (3 kcal/mol) and are comparable to the values also calculated in vacuo for some 2-substituted phenols forming intramolecular hydrogen bonds to the π-system.[37] They are about 1 kcal/mol smaller than the values obtained with the same functional but smaller basis set (6−31G(d)).[2] The predicted entropy changes due to thermal molecular motions are minimal, only 2.4 cal mol^{-1} K^{-1}, which

TABLE 1: Selected Geometrical Parameters of BINOL Isomers as Calculated with the PC Model Using Bondi's Radii to Bulid a Cavity

		bond lengths[a]			bond angles		dihedral angle		
	ε	(O)H···A[b]	O−H	C−C′	C−O−H	O−H···A	C(CC′)C′	OO′	dipole moment[g]
cc	1	2.337	0.975	1.498	109.0	113.3	91.4	3.814	1.274
	2.228[d]	2.347	0.975	1.498	109.4	112.8	91.4	3.812	1.497
	8.93	2.361	0.976	1.498	109.9	112.1	90.5	3.790	1.641
	36.64	2.370	0.976	1.498	110.3	111.6	89.9	3.777	1.606
Exp.[e]		2.439	0.938	1.500	114.9	115.2	88.3	3.805	
		2.321	0.973		105.7	107.1			
Exp.[f]		2.402	0.931	1.494	111.0		76.7	3.413	
		2.387	0.830		105.9				
ct	1	2.341	0.974	1.497	108.9	113.3	89.0	3.684	2.933
			0.970[c]		110.0				
	2.228[d]	2.348	0.974	1.497	109.3	112.8	90.3	3.719	3.406
			0.971[c]		110.1				
	8.93	2.356	0.976	1.497	109.6	112.4	89.0	3.684	3.908
			0.973[c]		110.2				
	36.64	2.363	0.976	1.497	110.0	111.9	88.8	3.680	4.075
			0.973[c]		110.1				
Exp.[h]		2.412	0.962	1.502	111.7	109.6	92.1	3.791	
			0.953[c]		112.6				
tt	1		0.969	1.495	109.7		88.3	3.607	1.451
	2.228[d]		0.971	1.495	109.9		88.0	3.602	1.692
	8.93		0.972	1.495	110.0		88.1	3.603	1.847
	36.64		0.973	1.496	110.0		86.4	3.558	1.849
Exp.[i]			0.961	1.487	120.9		94.5	3.745	
			0.979		110.1				

[a] Bond lengths in Å, angles in degrees. [b] Defined as the distance of a hydroxyl hydrogen atom to the nearest carbon atom, which happens to be a part of the central CC′ bond belonging to the other half of the molecule. [c] The hydroxyl group not participating in the intramolecular H-bond. [d] Optimized PCM values for a given solvent (ε = 2.228 − CCl_4; ε = 8.93 – CH_2Cl_2; ε = 36.64 − CH_3CN). [e] Crystal structure of rac-BINOL[4] with molecules without C_2 symmetry. [f] The values for (*R*)-(+)-BINOL[4] are different. [g] In Debyes. [h] Crystal structure of the BINOL-acetone inclusion compound consists of *ct* isomers.[5] [i] Crystal of the BINOL-THF inclusion compound is made of *tt* isomers.[5]

TABLE 2: Electronic Energy Differences, ΔE, Free Energy Differences with Thermal Corrections Included, $\Delta G'$, and also with the Non-Electrostatic Contributions Included, ΔG

ε	E_{cc}[a]	$\Delta E_{tt\text{-}cc}$	$\Delta E_{ct\text{-}cc}$	$\Delta G'_{tt\text{-}cc}$	$\Delta G'_{ct\text{-}cc}$	$\Delta G_{tt\text{-}cc}$	$\Delta G_{ct\text{-}cc}$
1	−921.064129	7.10	3.86	5.95	3.04	5.95	3.04
2.228	−921.072404	5.12	2.66	4.44	1.78	4.58	1.85
8.93	−921.081197	2.68	1.20	2.37	0.53	2.45	0.57
36.64	−921.084068	1.37	0.47	0.89	−0.31	0.99	−0.26

[a] Energies are in hartrees, differences are in kcal mol^{-1} (1 hartree = 627.510 kcal mol^{-1}).

is expected for the systems with an intramolecular H-bond. The energy of the intramolecular H-bond should not be far from the isomer enthaply difference $\Delta H_{ct\text{-}cc}$=3.71 kcal mol^{-1} since the geometries of the *cc* and *ct* or *tt* isomers are rather similar (Table 1). The energy differences $\Delta E_{ct\text{-}cc}$ and $\Delta E_{tt\text{-}ct} = \Delta E_{tt\text{-}cc} - \Delta E_{ct\text{-}cc}$ (Table 2) are not equal, which might be accounted for not only by the small differences in bond lengths and angles between the isomers but also by a cooperativity between the two H-bonds.

In order to obtain the height of potential barriers separating the isomers, the potential energy surface was scanned by fully optimizing the geometries keeping, however, the two dihedral angles C(CO)H, $\varphi_1 = \angle$(C1,C2,O,H) and $\varphi_2 = \angle$(C1′,C2′,O′,H′), fixed. The BINOL potential energy $V(\varphi_1,\varphi_2)$ is then a symmetric function of the two angles, $V(\varphi_1,\varphi_2) = V(\varphi_2,\varphi_1)$, and it is enough to explore only the area $-\pi \le \varphi_1 < \pi$ and $\varphi_2 < \varphi_1$. As expected, using the same functional and slightly larger basis set (6−31+G(d) instead of 6−31G(d)2[2]) we have obtained similar values for the isomerization barriers involving the OH rotations. While exploring the potential energy surface in such a way, the angle between the two naphthyl moieties takes the values between 62° and 103°. The deviation from the equilibrium value of 90° (Table 1) is 28° with the hydroxyl groups closer to each other, and only 13° when they are moved away from each other. The potential energy is thus weakly dependent on that angle around the minimum (the region of weak dependence must be defined as the one within which the planarity around the carbon atoms C1 and C1′ is kept). This will enable an easier formation of intermolecular H-bonds with solvent molecules because of the increase of the (O)H···A distance (Table 1), i.e., weakening of the O−H···π bond. The minimum energy path connecting *cc* and *ct* is the one along which one of the two OH groups barely moves while the other rotates. The transition state is reached when the latter is almost perpendicular to the naphthyl to which it is bonded. The main difference between the two transition states (Table 3) is the relative position of the two hydrogen atoms. The length of the central CC′ bond remains 1.497 Å in all cases. The other practically insensitive quantities are the bond lengths O−H and O′−H′ (0.974 ± 0.001 Å and 0.972 ± 0.001 Å, respectively) and the angles ∠C2−O−H and ∠C2′−O′-H′ (109.7 ± 0.5 and 110.8 ± 0.2 degrees, respectively). The normal mode having the imaginary frequency is the CO torsion involving the hydroxyl group that is perpendicular to the naphthyl plane. Thus,

TABLE 3: Electronic Free Energy Differences and Selected Geometrical Parameters of BINOL Transition States As Calculated with the PCc Model Using Bondi'S Radii to Bulid a Cavity[a]

	ε	$\Delta E_{TSi\text{-}cc}$	HH′	∠C(CO)H	∠C′(C′O′)H′	∠C(CC′)C′	μ
TS1	1.0	7.39	3.240	6.0	−99.3	87.6	1.848
	2.228	6.53	3.267	4.7	−95.8	90.0	2.033
	8.93	5.50[b]	3.293	2.6	−91.3	92.9	2.237
	36.64	4.94[b]	3.190	1.0	−89.4	91.1	2.311
TS2	1.0	6.88	4.117	−3.8	102.0	88.5	2.607
	2.228	6.08	4.085	−3.2	98.4	87.4	3.025
	8.93	5.12[b]	4.129	−1.6	94.2	88.9	3.547
	36.64	4.59[b]	4.075	−0.6	88.9	87.1	3.699

[a] Bond lengths are in Å, angles in degrees, dipole moment in Debyes, and energy differences in kcal mol^{-1}. [b] The best structures optimized with respect to forces but not to displacements and subsequently used to calculate frequencies. Any of the four structures has only one imaginary frequency. Fully optimized structures have also been obtained by using an order of magnitude weaker convergence criteria, but are not discussed here.

TABLE 4: Geometrical Parameters and Formation Energies for BINOL Trimers

	AN···cc···AN	AN···tt···AN
O−H[a]	0.9804	0.9762
N···H	2.0090	2.0200
O···N	2.9047	2.9877
∠(O,H,N)	150.8	170.8
∠(H,N,C)	155.5	166.2
∠(C,O,H)	114.2	111.0
∠(O,H,N,C)	−114.6	2.8
∠(N,H,O,C)	161.2	−167.5
∠(C,O,N,C)	63.3	−164.6
ΔG_v[b]	−5.54	−10.73
ΔG_{solv}[c]	3.38	−6.35
ΔG_s[d]	7.86	−1.44
$\Delta\nu$OH[e]	91	114

[a] Bond lengths are in Å and angles in degreees. [b] Free energy of formation in vacuo. [c] An estimate for the free energy of solvation for the complexes AN···*cc*···AN and AN···*tt*···AN in acetonitrile. [d] Free energy of formation in acetonitrile as solvent (single point calculations; for details see text). All energies are in kcal mol^{-1}. [e] The mean value of the scaled OH stretching wavenumber shifts (cm^{-1}) in vacuo upon H-bond formation.

any path from *cc* to *tt* not including *ct* is far more energy demanding. For the transition state TS1, the barrier height in vacuo from the *cc* side is 7.39 kcal mol^{-1}, while from the *ct* side nearly half of it, 3.52 kcal mol^{-1} (Tables 2 and 3). The analogous values for the transition state TS2 are 6.88 and 3.01 kcal mol^{-1}, respectively. We present here only data for the pair of isomers *cc* → *ct* because the conformational change almost always starts with the *cc* isomer. A conformation with the intramolecular H−O···H−O hydrogen bond also occurs on the potential energy surface but is energetically unfavorable since a rather small internaphthyl angle would be required leading to the enhanced repulsion of the hydrogen atoms at positions 8 and 8′.

In order to get an idea about the energetics and geometries of H-bond formation that certainly takes place in solvents such as AN, THF, and DMF, some modeling of H-bonded trimers have been perfomed (Table 4). Of the three solvents, AN was the most suitable because of its quasi-linear molecular shape. The full geometry optimization of both trimers, AN···*tt*···AN, and AN···*cc*···AN, in vacuo at the same level of theory as above gave stable structures (no imaginary frequencies) possessing C_2 symmetry. The trimer AN···*tt*···AN has nine normal modes with wave numbers below 50 cm^{-1}, while for AN···*cc*···AN that number is seven. Therefore, the usual way of calculating thermal motion contributions to the free energy could not be applied, and only the electronic energies differences with all nonelectrostatic contributions included and after taking into account the BSSE are used here. As expected, the trimer AN···*tt*···AN with pure intermolecular H-bonds is predicted to be more stable in vacuo.

3.2. Influence of the Solvent on the Conformational Energies and Vibrational Frequencies. The molecular structure is not that sensitive on the dielectric (Table 1). However, in single-point calculations in vacuo (not shown) of the solvent optimized geometries, even these small differences produce the energies differing by several kcal mol^{-1}. Interactions with solvent might substantially decrease the barrier heights shown here as electronic free energy differences (Table 2). Thus, even under standard conditions the conformational equilibrium is expected to take place, possibly with changed conformational preference.

The *ct*-isomer either free or in solution possesses the largest dipole moment (Table 1) and is, in comparison with the other two isomers, additionally stabilized in polar solvents by dipole−dipole interactions. However, this is not enough to change the order of the relative stability of the isomers except in very polar solvents. For all three conformations, the dipole moment is increased by the solvent field (by 0.38 D for *cc* and *tt* and 0.97 D for the *ct* conformer in CH_2Cl_2). At the same time, the increase between the conformers *tt* and *cc* is roughly solvent independent (≈ 0.20 D). This, of course, is not true for the *ct*-*cc* differences that increases markedly with the solvent polarity. In other words, the dipole moment of the *ct* isomer is much more sensitive to the changes in permittivity than of the other two isomers. The difference $(ct\text{-}cc)_{solv} - (ct\text{-}cc)_{vacuum}$ measures the solvent induced changes in the dipole moment, and it amounts up to one-third of the total change in a highly polar solvent, the rest being due to the changed relative positions of the two hydroxyl groups.

In estimating the relative stability of the conformers in a given solvent, the relevant quantity is the free energy difference that includes all the nonelectrostatic contributions (cavity and dispersion-repulsion terms) and thermal corrections due to the molecular motions at a given temeperature (Table 2). Since the molecule is in the cavity its translational and rotational motions are restricted, the corresponding thermal corrections cannot be evaluated the same way as for a free molecule, and the enthalpies of solvation cannot be straightforwardly obtained. However, there is some cancelation of errors when the conformational differences are calculated in a given solvent, especially due to the small changes in cavity shape and volume and moments of inertia from one conformer to the other. The energy differences $\Delta E_{ct\text{-}cc}$ and $\Delta E_{tt\text{-}ct}$ are not equal, and their ratio is decreasing with the solvent permittivity, i.e., in highly polar medium, the

ct isomer is closer in energy to the *tt* isomer than to the *cc* isomer. Using the thermodynamic cycle for the two isomers in the gas phase and solution, the difference between the solvations energies for the two isomers can be correctly predicted, for example, $(\Delta G_{ct})_{solv} - (\Delta G_{cc})_{solv} = (\Delta G_{ct\text{-}cc})_{gas} - (\Delta G_{ct\text{-}cc})_{solution}$. According to the calculated data (Table 2), this is positive for all solvents indicating stronger stabilization of the isomer less stable in the gas phase.

Concerning the reaction paths connecting *cc* and *ct* isomers, from the heights of the barriers the TS2 turns out to be the preferred channel both in the gas phase and within the continuum (Table 3). Since the barrier height differences are not that large, a part of the *cc* isomers will be transformed following the path that includes TS1. The calculated dipole moments of BINOL isomers and their transition states are fully in accord with this picture.

3.3. Gas Phase and Solid State Spectra. With 36 atoms, a BINOL molecule possesses 102 vibrational degrees of freedom. In the cases of *cc*- and *tt*-isomers, it has C_2 symmetry and the normal modes are distributed as 52A+50B. The central CC′ stretching, νCC′, is totally symmetric, as is the internaphthyl CC′ torsion, τCC′, while all the other internal oscillators occur in symmetric and antisymmetric combinations. Thus, there are two hydroxyl group stretching modes, νOH, one in-phase (symmetric), νOHA, and the other out-of-phase (antisymmetric), νOHB, and analogously for the in-plane OH bendings, βOHA and βOHB. The out-of-plane OH bendings are described by the torsions around the CO bonds, τCOA and τCOB. Other internal motions of interest are the CO stretchings, νCOA and νCOB, the in-plane CO bendings, βOCA and βOCB, the out-of-plane CO bendings, γCOA and γCOB, and analogously for the CC′ bond, the in-plane bendings, βCC′A and βCC′B and the out-of-plane bendings, γCC′A and γCC′B. It is important to notice that an internal coordinate that would be describing the interaction between the O−H bond and the π-cloud of the neghboring naphthyl moiety is missing here.

A dimer model of a BINOL molecule made of two *cis*- or *trans*-2-naphthol molecules can be again considered in order to explain some characteristics of the BINOL spectrum. The dimer is not weakly coupled because the two halves of BINOL molecule are not only covalently bonded but also interact with each other through the OH···π H-bonds. Since the enthalpy difference between the two 2-naphthol isomers is less than 1 kcal mol^{-1}, the observed spectra of 2-naphthol[18,38] are superpositions of equally weighted isomer spectra. Therefore, the comparison with BINOL is not that straightforward and will not be used further on.

The gas phase IR spectrum[18] should obviously be interpreted as belonging dominantly to the *cc*-isomer. The pair of OH stretching bands, one very weak at 3648 cm^{-1} and the other strong at 3562 cm^{-1}, are typical for the systems with the internal OH···π H-bond. Since the conformational change is a thermally activated process, there is a certain percent of BINOL molecules even in the gas phase, which are not *cc*-conformers. Most probably only the *ct* isomers are observed because the *tt* isomer has the highest energy. From the relative heights of the OH absorption peaks in the gas phase spectrum ($\approx$ 0.033), an approximate free energy difference of $\Delta G \approx 2.03$ kcal/mol at $T \approx 300$ K can be deduced assuming that the molar absorption coefficient for the *cc* isomer is nearly two times that of the *ct* isomer. The OH torsional frequency in *ortho*-substituted phenols has been used in the determination of the enthalpy difference between two conformers,[39] and for 2-phenyl-phenol diluted in cyclohexane, the value of 2.73 kcal mol^{-1} (not so certain as the values for other studied molecules) was obtained. It was estimated that most probably it was between 1−3 kcal mol^{-1}, with the barrier from the side of the more stable isomer of up to 5 kcal mol^{-1}. These values favorably compare with the free energy differences (Table 2) and barrier heights (Table 3) calculated for non H-bonding solvents.

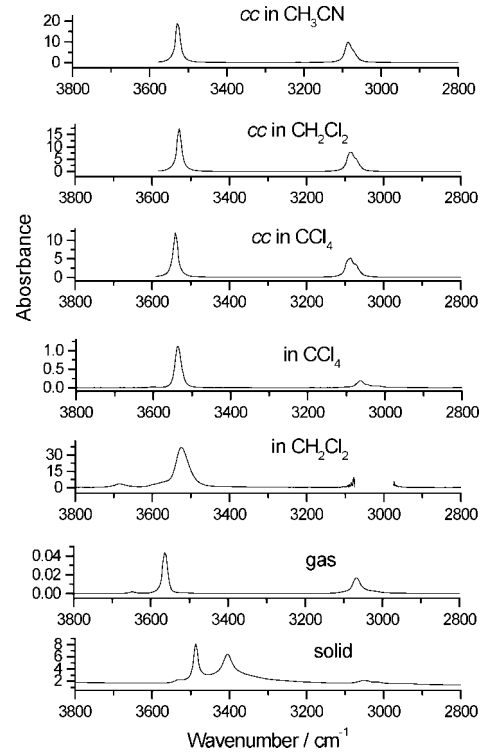

Figure 2. Calculated OH stretching region of the *cc* isomer and observed spectra in H-bond nonaccepting solvents, gas phase, and solid.

The observed wavenumbers and relative intensities in the gas and solid phases are listed in Table S1 (Supporting Information), together with the results of calculations at the B3LYP/6−31+G(d) level of theory. When the calculated *cc* spectrum is compared with the gas phase spectrum, one generally finds reasonable agreement not only of wavenumbers but also of the IR intensities (Figures 2 and 3), as long as the vibrations of the naphthyl groups are considered (the same holds when the gas phase spectrum is compared to the solid state spectrum). The calculated upshift of the νOH stretching wavenumber of the *ct*-isomer (3627 cm^{-1}) relative to the *cc*-isomer (3531 cm^{-1}) is 96 cm^{-1}, in agreement with the observed value of 86 cm^{-1}. The fact that the calculated νOH···π stretching is also upshifted by 34 cm^{-1} with respect to the νOH vibrations of the *cc* isomer is an indication that now the OH···π H-bond is toward a somewhat different π-system. The slight asymmetry of the 3562 cm^{-1} gas band from the high wavenumber side might thus be interpreted as due to the νOH···π vibration of the *ct* isomer (the symmetric vibration νOHA of the *cc* isomer occurs at a lower wavenumber and is predicted to have practically zero IR intensity).

In the racemic BINOL crystal, only *cc*-molecules are linked around a 2_1 axis through hydrogen bonds between the hydroxyl groups. The crystal has a space group symmetry *Iba2* (C_{2v}^{21}) with $Z = 8$ molecules in the unit cell[4] meaning that there are $Z = 4$ molecules in the primitive unit cell. To roughly describe the vibrations of hydrogen bonds, it is enough to consider a one-dimensional chain of a 2_1 symmetry with a repeating unit having $z = 2$ molecules. The two oxygen atoms involved in the hydrogen bond between the neighboring molecules are at the

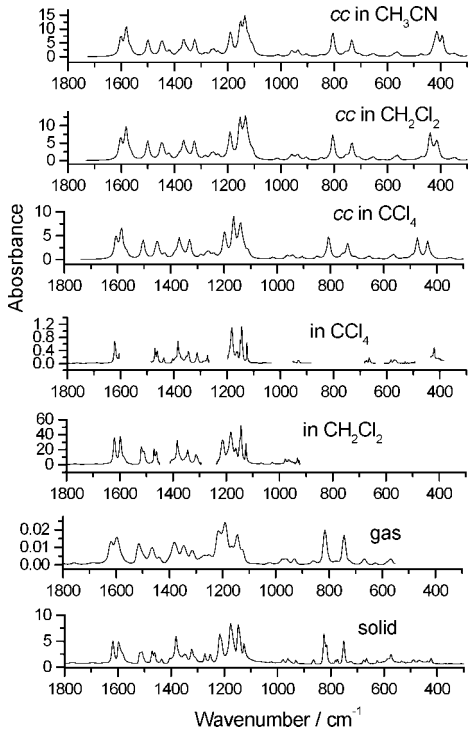

Figure 3. Calculated spectra below 1800 cm^{-1} of the *cc* isomer and observed spectra in H-bond nonaccepting solvents, gas phase, and solid.

distance of 2.852 Å (this is much closer than the intramolecular OO′ distance (Table 1)), while the OH···O angle is 141.0°. Thus, in each molecule both hydrogens are hydrogen bonded to the neighboring π-cloud, and both take part in the intermolecular hydrogen bond. In other words, BINOL is amphipathic, as are other alcohols. This, of course, suggest a possibility of BINOL dimerization in solution. The two IR bands due to hydrogen bonding are therefore seen with different characteristics. The one at 3487 cm^{-1} is strong and sharp and the other at 3404 cm^{-1}, also strong but weaker, broadened in the lower half as if it emerges from one weaker and another broadband centered at around the same wavenumber. As already mentioned above, a single BINOL molecule exhibits two OH stretching modes, νOHA and νOHB, the former having practically zero intensity, with the predicted wavenumber splitting of only 3−5 cm^{-1}. In the crystal, the two OH oscillators on a single molecule are different: one is taking part in the intermolecular H-bond as an acceptor, while the other is a bifurcated donor. Therefore, the observed splitting amounts to 83 cm^{-1}, which is comparable to 117 cm^{-1}, i.e., to the gas to crystal shift of the νOHB band with respect to the arithmetic mean of the two crystal bands. The broader band at 3404 cm^{-1} should thus be associated with the bifurcated OH oscillator. In similar systems having a hydroxyl group attached to the aromatic core but without an intramolecular H-bond, a strong absorption is found at 3654 and 3650 cm^{-1},[18] in the gas phase of 2-naphthol and phenol, respectively. The corresponding bands are observed at 3283 and 3225 cm^{-1} in crystalline 2-naphthol and phenol, respectively. In both cases, there are intermolecular H-bonds between the symmetricaly nonequivalent molecules. For each gas phase band in the regions 1650−1250 and 1100−550 cm^{-1}, there is a doublet of closely lying crystal bands.

The two bands dominating the spectra around 1600 cm^{-1}, at 1618 and 1598 cm^{-1}, are attributed to the naphthyl CC stretchings, while the bands below 1000 cm^{-1}, at 814 and 746 cm^{-1} (gas), are due to the naphthyl out-of-plane CH bendings. Both pairs of bands keep their characteristics for *ct*-isomer but not for the *tt*-isomer, indicating that the latter rearly occurs in the gas phase and is absent in the crystal phase, as is also known from the crystal structure.[4] In the gas phase, two triplets of bands are observed from 1550 to 1300 cm^{-1}. In the condensed phase, each of the bands is still present and actually turns out to be a doublet. They all can safely be interpreted as in-plane deformations of the naphthyls (Table S1, Supporting Information).

What is observed in the 1250−1050 cm^{-1} region is according to the calculated *cc* spectrum due to the CO sttretchings and in-plane OH bendings, i.e., the kind of motion that is expected to be sensitive to the isomerism. The redistribution of intensities takes place on going from gas to crystal phase with the band positions unchanged except in one case, i.e., the strongest band in crystal is at 1147.6 cm^{-1} and not at 1190 cm^{-1} (Table S1, Supporting Information). The modes of the *cc*-isomer at 1290.0 (A) and 1174.3 (B) cm^{-1} have the character of the OH in-plane bending, βOH, and that part of the spectrum of the other two isomers should thus look different. The latter is predominantly the OH in-plane bending motion coupled with the CO stretching and might serve as diagnostic of the isomerization equilibrium. It is assigned to the mentioned pair of the strongest bands. The corresponding modes of the *tt*-isomer are found at 1269.6 and 1179.3 cm^{-1}, and obviously, only the downshift of ∼20 cm^{-1} for the former might be measurable.

There is no such mode of the *cc* isomer, which would predominantly have the C1C1′ stretching character. The C1C1′ stretching contributes to the 1290.0 (A), 1047.2 (A), and 187.0 (A) cm^{-1} modes, and their assignment to the observed Raman bands of crystal[9] is not straightforward. (The bands recorded in 3 M NaOH aqueous solution most probably belong to the $BINOL^{2-}$ anion and will not be considered here.) These values are all below 1300 cm^{-1}, which was taken[8] as the lower limit (obtained in a BPW91/6−31G(d) model) for the modes partially having the C1C1′ stretching character. The two bands, at 666 and 570 cm^{-1}, of the lowest group of bands in the gas phase spectrum are also present in the crystal spectrum as well resolved doublets. They may be assigned to the in- and out-of-plane deformations of the naphthyl carbon skeleton. Other types of internal oscillators such as the torsions around the CO bonds bearing even larger significance (the conformational change is actually defined by the changes in the corresponding torsional angles) lie below 500 cm^{-1} and unfortunatelly could only be vaguely observed.

It is surprising to see how well the Raman spectrum of solid BINOL[9,10] is reproduced at the B3LYP/6−31+G(d) level. Around 1600 cm^{-1}, the observed Raman bands are all due to the naphthyl CC stretchings, and no contribution of the CO stretchings is found here. The strongest Raman band of solid BINOL at 1381 cm^{-1} is not due to the symmetric CO stretching calculated at 1205.2 cm^{-1}, but rather due to the CC bond stretchings of the central parts of the naphthyl moieties calculated at 1358.3 cm^{-1}. A weak and asymmetrically broad IR band at 467 cm^{-1} is observed in solid BINOL that is missing in all solution spectra, as will be discussed below. There is no Raman band at that position. The closest bands are at 490 and 440 cm^{-1}, both having their counterparts in IR (Table S1, Supporting Information).

The observed shifts from gas to crystal are practically all up to 1% (positive for the in-plane naphthyl modes and negative for the out-of-plane naphthyl modes) except for the vibrations that includes the motions of the hydroxyl groups. The largest shift of even 30% is predicted for the lowest mode that is

actually pure internaphthyl torsion, i.e., small amplitude internal rotation of BINOL.

3.4. Spectra in Hydrogen Bond Nonaccepting Solvents. The discussion in this section is limited to the experimental results with the three H-bond nonaccepting solvents, i.e., carbon tetrachloride, chloroform, and dichloromethane. In calculations, three different values of the dielectric constant, 2.228, 8.93, and 36.64, corresponding to carbon tetrachloride, dichloromethane, and acetonitrile, respectively, were chosen to examine the solvent effects within the model of the polarizable continuum (Table 5).

The stabilization of different isomers by dielectric solvent effects is evident (Table 2). As evidenced from the recorded spectra and in agreement with calculations, the stability order at room temperature does not change when the BINOL molecule is introduced into dielectric of low permittivity that is also a non-H-bonding accepting solvent. Nevertheless, it is essential to search for the spectral indications of the isomerization equilibrium in solution spectra not only around 3500 cm^{-1} where the OH stretchings whether hydrogen bonded or not give rise to the observed bands, but also in the 1300−1100 cm^{-1} interval where the in-plane OH bendings are expected and from 500 to 300 cm^{-1} where the CO torsion (also called OH torsions) are observed. An idea in what direction the intensity changes might take place can be gained from the calculated spectra when compared with each other (Figures 2 and 3). Thus, for example, the absence of the doublet around 1600 cm^{-1} would indicate the prevalence of the *tt*-isomer as would the presence of the relatively strong and barely resolved doublet around 310 cm^{-1}. The greatest intensity change upon transition from gas to solution in dichloromethane is predicted for the βOH vibrations, and the band at 1100 cm^{-1} should actually dominate that spectral region. However, this is not observed. The resemblance of the *cc*- and *ct*-isomer spectra to that of the gas phase suggests an equilibrium between the two isomers.

The formation of intermolecular hydrogen bonds with solvent molecules is excluded here, except possibly for chloroform. Therefore, the molecular conformation of BINOL with respect to the two dihedral angles ∠C(CO)H is expected not to change in CCl_4, $CHCl_3$, and CH_2Cl_2 solutions. However, a weak band at 3591 ± 10 cm^{-1} invariably assigned to free OH groups occurs here (Table 5). In other words, an equilibrium we are dealing with is between a *cc* isomer surrounded with solvent molecules but not hydrogen bonded to any of them and the *ct* isomer again not hydrogen bonded to one of them and also surrounded with other solvent molecules. From the observed ratio of the two bands at room temperature, the enthalpy difference is estimated to be around 1−2 kcal mol^{-1}, which overlaps with the range 0.4−1.5 kcal mol^{-1} established by means of temperature dependent measurements on *ortho*-trityl phenols.[19] Assuming that the calculated free energy differences (Table 2) give reasonable estimates of the real values, the entropy terms also including the electrostatic contribution thus seems to be rather small (the calculated entropy difference between the isomers due to thermal motions amounts only up to 0.01 kcal mol^{-1} at 298 K).

The observed IR bands of BINOL in solutions are listed in Table 5. All of the calculated wavenumbers are depicted in order to make it obvious that the correspondence between the observed and calculated values can only be roughly established to within the spectral regions. By giving only those of the calculated values[10] that have been assigned to the observed values, an impression is brought about that the agreement looks better than it actually is. The normal mode descriptions in this article are based on the calculated potential energy distributions in terms of internal coordinates and not on the visual inspection of the calculated Cartesian displacements.[10] As shown, BINOL in carbon tetrachloride, chloroform, and dichloromethane exhibits a strong band at 3537, 3531, and 3526 cm^{-1}, and another much weaker one at 3602, 3587, and ∼3585 cm^{-1}, respectively. 2,2′-Dihydroxybiphenyl is structurally similar to BINOL, but unlike it, it strongly absorbs at 3556 cm^{-1},[12] i.e., 20 cm^{-1} higher. The weak band at 3602 cm^{-1} in CCl_4 does belong to BINOL by analogy with a band at 3610 cm^{-1} that is characteristic of the free OH group of phenols[40] and 2-phenylphenol and 2,2′-dihydroxybiphenyl[12] in CCl_4. Furthermore, when recorded in $CHCl_3$ and CH_2Cl_2, phenol absorbs at 3598 and 3582 cm^{-1}, respectively. 2-Naphthol absorptions are found at 3609 cm^{-1} (CCl_4), 3595 cm^{-1} ($CHCl_3$), and 3578 (CH_2Cl_2) cm^{-1} (Table S2, Supporting Information). The weak BINOL band at 3602 cm^{-1} in CCl_4 should belong to *ct*-isomers because they transform back to *cc*-isomers with far greater probability than to *tt*-isomers. The stronger bands are assigned to the νOH modes of the hydroxyl groups involved in OH···π hydrogen bonds. Its symmetry in CCl_4 is in accordance with the calculated negligible intensity of the νOHA normal mode. However, the circular dichroic IR spectra[7] indicated the presence of the band doublet, and after the band deconvolution, the splitting of 14 cm^{-1} has been obtained between the two bands of comparable intensity. This is roughly in agreement with the calculated one of 4−5 cm^{-1}, but the calculated IR intensities do not support this view (Table 6). The small frequency difference reflects a negligible coupling of the two OH oscillators, which is in accordance with the fact that the two OH groups are only indirectly coupled. In $CHCl_3$, the 3531 cm^{-1} band is obviously asymmetric with a longer tail to the low frequency side. At higher concentrations, the tail reveals the presence of yet another very broad and weak band at ∼3440 cm^{-1}. The band asymmetry can be satisfactorily recovered by fitting it to two Lorentzians having maxima at 3535 and 3521 cm^{-1}, with the lower frequency component of higher intensity. This asymmetry might be attributed to the unresolved stretchings of the OH groups involved in intermolecular hydrogen bonds, i.e., to those BINOL molecules acting as chloroform proton acceptors. In CH_2Cl_2, the strong band at 3526 cm^{-1} is practically symmetric were it not for the very weak shoulder at ∼3585 cm^{-1}. In the vicinity, there is a weak and well resolved band at 3686 cm^{-1} corresponding to a higher order transition of BINOL, also found in other H-bonding nonaccepting solvents.

It is probably the right place here to examine the exact nature of the O−H···π H-bond, i.e., whether it is really an H-bond according to generally accepted spectroscopic criteria. The most dramatic evidence of forming an H-bond is the IR intensity enhancement for an order of magnitude of the νOH stretching mode. Only the calculated molar absorption coefficients for the BINOL isomers are available (Table 6), and obviously, the formation of the O−H···π bond is not accompanied by that great sensitivity of the dipole moment on the OH stretching coordinate. The reason for the wavenumber shift of 60−90 cm^{-1} (2−3%) might also be weak anharmonic modulation by one or a group of slower molecular vibrations. The (O)H···A distance (Table 1) greatest changes are induced by the normal modes partaking of βCO bending motion and calculated at 358 and 297 cm^{-1} (Table 5). This also explains why the widths of the O−H···π bands are an order of magnitude smaller than the widths of the O−H···Y (Y = N, O) bands in H-bond accepting solvents. In the latter case, particularly when the H-bond is

TABLE 5: Observed Wave Numbers of BINOL in Non-H-bonding Solvents and Calculated PCM Wave Numbers of the *cc*-Isomer for $\varepsilon = 8.93$ (Dichloromethane)

observed				calculated in CH_2Cl_2					
IR gas[a]	in CCl_4	in $CHCl_3$	in CH_2Cl_2	*cc*-BINOL[b]	IR int.[c]	Symm.	P.E.D.[d]		
3648.0 w	3602.0 vw	3586.9 w	3585.0 vw,sh						
3562.0 s	3537.2 vs	3531.4 s	3525.6 s	3530.8	vs	1B	100 **ν OH**		
				3526.6	vw	1A	100 **ν OH**		
				3092.6	vw	2B	98 νCH		
				3092.3	vw	2A	98 νCH		
3066.0 m	3062.7 m	3063.0 m,sh		3062.7	vw	7A	91 νCH		
3013.0 w,sh	3028.0 w,sh			3062.7	vw	7B	90 νCH		
2959.0 vw		2975.9 m,?							
		2696.3 w							
1956.0 vw									
1909.0 vw									
1826.0 vw									
1756.0 vw									
1683.0 vw	1687.1 w,?	1683.7 w,?							
1618.0 s	1621.0 m	1620.1 s	1620.1 s	1602.6	vw	8A	50 νCC		
				1602.4	w	8B	49 νCC		
1598.0 s		1597.9 s	1597.4 s	1582.7	w	9A	61 νCC		
				1580.1	w	9B	55 νCC		
		1583.0 w,sh	1583.0 w,sh	1572.2	vw	10A	49 νCC		
				1564.5	vw	10B	52 νCC		
1514.0 s		1517.4 m	1517.9 m	1501.7	vw	11A	26 νCC		
1500.0 w,sh		1509.0 m,sh	1510.0 w	1499.4	vw	11B	35 νCC		
1466.0 m	1470.1 m	1470.6 m	1470.6 m	1450.4	w	12A	29 βCH		
	1461.9 m	1461.9 m	1461.9 m	1443.5	vw	12B	31 βCH		
1437.0 w	1437.3 m	1437.3 w	1436.9 w	1422.8	vw	13A	49 βCH		
		1433.0 w,sh	1430.0 w,sh	1420.4	vw	13B	37 βCH	11 νCC	
	1404.1 w	1405.0 w	1405.1 w						
				1382.9	vw	14A	18 βCH		
1382.0 s	1384.8 m	1384.8 s	1384.3 m	1366.1	w	14B	53 νCC		
	1377.0 sh	1379.0 m,sh	1380.0 w,sh						
	1353.0 vw	1353.0 w,sh	1354.0 w,sh	1354.8	vw	15A	66 νCC		
1346.0 w	1345.3 w	1344.8 w	1345.7 w	1347.7	vw	15B	70 νCC		
1314.0 w	1313.0 w	1313.9 w	1313.4 w	1326.1	vw	16A	48 νCC		
				1324.3	vw	16B	44 νCC		
	1288.0 vw	1287.0 vw		1285.4	vw	17A	34 β**OH**	19 ν**CC′**	
1268.0 vw	1274.0 w	1273.9 m		1262.3	vw	17B	20 νCC	16 ν**CO**	12 β**OH**
				1252.9	vw	18A	32 βCH	23 αCC	
1252.0 vw				1235.9	vw	18B	36 βCH	11 νCC	
				1197.0	vw	19A	38 νCC	21 βCH	
				1195.5	vw	19B	42 νCC	15 βCH	
1216.0 m			1212.1 m	1190.4	m	20A	18 ν**CO**	12 νCC	
1190.0 s	1181.8 m	1182.3 s	1183.2 s	1154.3	m	20B	35 β**OH**	18 ν**CO**	18 βCH
1166.0 w	1161.5 w	1164.0 w	1164.0 w	1142.2	vw	21A	41 βCH		
	1150.0 w	1150.0 m,sh	1150.0 w,sh						
1146.0 m	1144.2 m	1144.7 s	1144.2 s	1133.3	w	22A	55 βCH		
				1132.5	w	21B	35 βCH	12 β**OH**	
1124.0 w	1125.4 w	1125.9 w	1125.9 w	1128.4	vw	22B	47 βCH	11 νCC	
				1121.3	w	23A	14 β**OH**	14 βCH	11 νCC
				1107.2	w	23B	16 βCH		
1067.0 vw		1069.0 vw	1080.0 vw						
		1040.0 vw		1042.9	vw	24A	33 αCC	11 ν**CC′**	
1024.0 vw		1027.0 vw	1030.0 vw	1014.0	vw	24B	47 νCC		
				1013.9	vw	25A	48 νCC		
				963.7	vw	25B	109 γCH		
972.0 w		977.8 w	977.8 w	963.5	vw	26A	109 γCH		
				960.3	vw	26B	19 νCC	14 αCC	14 ν**CO**
960.0 w		966.8 w	964.8 w	949.7	vw	27A	81 γCH		
		955.0 sh	954.0 w,sh	948.8	vw	27B	94 γCH		
				937.3	vw	28A	20 αCC	15 ν**CO**	
				931.4	vw	28B	81 γCH		
930.0 m	930.6 w	931.1 w	931.1 w	931.4	vw	29A	78 γCH		
				905.2	vw	29B	86 αCC		
858.0 w		865.0 w	866.0 w	849.2	vw	30A	86 γCH		
				848.6	vw	30B	86 γCH		
				826.7	vw	31A	40 αCC	11 νCC	
814.0 s		821.1 m	821.6 m	805.9	w	31B	86 γCH	15 γ**CO**	
				805.5	vw	32A	86 γCH	15 γ**CO**	

TABLE 5 Continued

observed						calculated in CH_2Cl_2			
IR gas[a]	in CCl_4	in $CHCl_3$	in CH_2Cl_2	*cc*-BINOL[b]	IR int.[c]	Symm.	P.E.D.[d]		
776.0 w				773.4	vw	32B	20 τCC	14 νCC	
				757.4	vw	33A	144 τCC	16 γ**CC′**	
				753.8	vw	33B	109 τCC	15 γCH	
				734.9	vw	34B	81 γCH		
746.0 s				734.4	vw	34A	85 γCH		
720.0 w,sh				711.8	vw	35A	63 αCC		
				705.4	vw	35B	41 αCC	10 ν**CO**	
				662.6	vw	36B	76 τCC	44 γ**CO**	
666.0 w			676.0 w	661.7	vw	36A	76 τCC	45 γ**CO**	
626.0 w		626.8 w	626.8 w	651.9	vw	37A	61 αCC		
				616.9	vw	37B	83 αCC		
582.0 w,sh	584.0 w	584.0 vw	584.4 w	573.7	vw	38A	58 τCC	18 τCC	12 τCC
570.0 w	570.0 w, bd	571.8 vw, bd doublet	571.8 w, bd doublet	561.9	vw	38B	58 τCC	15 γ**CC′**	
534.2 vw[e]	531.2 vw	532.0 vw	531.0 vw	524.7	vw	39A	54 τCC	30 γ**CO**	
524.0 vw	521.8 vw	522.0 vw	522.7 vw	526.7	vw	39B	56 τCC	26 γ**CO**	
				519.9	vw	40A	65 αCC		
513.0 vw	504.5 vw	507.0 vw	507.2 vw	509.9	vw	40B	63 αCC		
487.9 vw,bd		484.6 w	484.6 w	494.3	vw	41A	45 τCC	32 β**CO**	
				473.5	vw	41B	31 αCC	19 β**CO**	16 τCC
467.0 vw,bd				440.5	m	42A	96 τ**CO**		
437.0 vw		436.7 m	436.8 m	425.8	vw	43A	40 αCC	14 τCC	
				425.5	vw	42B	33 αCC	15 τ**CO**	10 τCC
422.4 w	421.4 m	422.9 m	422.4 m	417.5	vw	43B	65 τ**CO**	15 αCC	
420.0 sh				413.2	vw	44A	84 τCC		
				410.4	vw	44B	61 τCC	18 τ**CO**	
372.2 vw			370.0 vw	358.1	vw	45A	16 β**CO**	14 γ**CO**	14 τCC
			357.0 vw	346.8	vw	45B	34 τCC	24 γ**CO**	
				335.3	vw	46A	16 αCC	14 γ**CO**	12 τCC
310.0 vw				296.6	vw	46B	28 β**CO**	11 αCC	
				230.1	vw	47A	70 τCC		
				227.7	vw	47B	72 τCC		
				186.5	vw	48A	16 αCC	14 β**CO**	11 ν**CC′**
				144.5	vw	49A	85 τCC		
				143.7	vw	48B	94 τCC		
				109.0	vw	50A	68 τCC		
				107.8	vw	49B	72 τCC		
				53.4	vw	51A	43 γ**CC′**	27 β**CC′**	12 τCC
				52.1	vw	50B	47 γ**CC′**	31 β**CC′**	15 τCC
				27.9	vw	52A	95 τ**CC′**		

[a] Ref..[18] [b] Wavenumbers are scaled by 0.9648. [c] s, strong; w, weak; v, very; m, medium; sh, shoulder; bd, broad. [d] Potential energy distribution in terms of internal symmetry coordinates. The contributions (shown only if not less than 10) of the same type are summed. They are not percentages, their relative magnitudes matter. For example, the modes 17A and 20B may be described as pure hydroxyl group modes. νCH, CH stretching; νCC, aromatic CC stretching; βCH, aromatic in-plane CH bending; αCC, aromatic CCC bending; γCH, aromatic out-of-plane CH bending; τCC, C(CC)C torsion; ν**OH**, OH stretching; ν**CC′**, C1C1′ stretching; ν**CO**, CO stretching; β**OH**, in-plane COH bending; γ**CC′**, out-of-plane C1C1′ deformation; β**CC′**, in-plane C1C1′ deformation; τ**CO**, C(CO)H torsion; β**CO**, in-plane CO bending; γ**CO**, out-of-plane CO bending. [e] This and the bands below belong to solid BINOL.

linear, the coupling between the O−H and O···Y stretchings is rather effective in producing strong and very broad absorption bands.

The linearity of the absorption intensity of the BINOL νOH and other bands versus concentration in the range between 0.02 and 0.08 mol dm^{-3} in all used solvents has been established within experimental error, and therefore, dimerization of BINOL molecules could have been neglected. The molar absorption coefficient E_m at the maximum of the νOH···π band has the value of 325 ± 8 dm^3 mol^{-1} cm^{-1} in dichloromethane, 248 ± 25 and 191 ± 18 dm^3 mol^{-1} cm^{-1} in chloroform and 607 ± 20 dm^3 mol^{-1} cm^{-1} in carbon tetrachloride (Table 6). The only reason for different values is the dependence of the molar absorption coefficient on the permittivity of the dielectric surrounding the molecule. In order to compare the calculated infrared intensities (reported in kmmol^{-1}), the integrated molar absorption coefficients must be measured. The increase with solvent polarity of the integrated molecular decadic absorption coefficient of the OH stretching band from CCl_4 to CH_2Cl_2 by 34.5 kmmol^{-1} is reproduced by the calculated value of 54.2 kmmol^{-1}. The triplet of bands around 1600 cm^{-1} shows similar intensity values for non-H-bonding solvents. However, while the observed intensities of the two bands at 1620 and 1597 cm^{-1} are equal, the calculated intensity for the latter is around 1.5 times greater than that for the former. This ratio is kept at higher values of permittivity. Quite oppositely, the experimental values in H-bonding solvents show that the former is more intense by the same factor. This obviously is a consequence of forming the intermolecular H-bonds. In DMF, the band at 1598 cm^{-1} is the weakest one.

Since the frequency of the OH stretching, νOH, serves as a measure of the hydrogen bond strength, a loose correlation between νOH and the frequency of the OH out-of-plane bending, τCO, could have been established[42] (generally, the lower νOH, the higher τCO). This type of torsional motion is observed for phenol at 306 cm^{-1} (the calculated wavenumber for phenol in

TABLE 6: Experimental and Calculated IR Intensities of the Selected *cc*-BINOL Transitions in Various Solvents

solvent	ε	$\tilde{\nu}Z_{calc}$[a]	log e•calc. integr. E_m[b]	$\tilde{\nu}_{obs}$	obs. integr. E_m[b]	obs. peak height E_m [c]	obs. fwhh[c]
CCl_4	2.228	*3609*[g]	*50*	3602			
		3550	*57*				
		3540	124	3537	148 ± 7	607 ± 18	17
		3535	0.1				
		1606	44				
		1586	63				
		1574	13				
		1126	17	1125	12 ± 0	305 ± 11	3
$CHCl_3$	4.90			3535[d]	61 ± 3	248 ± 25	29
				3521	99 ± 6	191 ± 18	18
				1620	38 ± 1	299 ± 9	13
				1597	37 ± 1	307 ± 10	8
				1585	14 ± 1	49 ± 3	8
CH_2Cl_2	8.93	*3590*[g]	*72*	3588	2.4 ± 0.2	8 ± 1	13
		3534	*88*				
		3530	178	3523.0	182.7 ± 1.1[e]	325 ± 8	36
		3526	0.3				
		1603	58	1620	38.0 ± 0.4	300 ± 7	8
		1583	92.5	1597	41.0 ± 0.3	305 ± 4	9
		1572	17	1584	8.2 ± 0.5	48 ± 3	12
THF	7.58			3296 [f]	496 ± 9	223 ± 9	178
				1621	40 ± 1	280 ± 13	9
				1598	22 ± 1	180 ± 8	8
				1589	31 ± 1	71 ± 5	25
				751	44 ± 2	344 ± 55	9
CH_3CN	36.64	*3583*[g]	*80*				
		3523	*101*				
		3527	200	3392 [f]	185 ± 15	62 ± 1	170
		3523	1				
		1602	63	1621	99 ± 8	62 ± 2	11
		1582	106	1598	49 ± 2	38 ± 1	8
		1572	20	1587	31 ± 1	15 ± 1	18
DMF	36.7			3202	1251 ± 101	296 ± 9	290
				1622	71 ± 4	304 ± 11	14
				1598	12 ± 1	96 ± 2	8
				1585	47 ± 1	147 ± 3	20

[a] In cm^{-1}. [b] In mol^{-1} km. The calculated intensities should be multiplied by log e before being compared to the experimental integrated molecular absorption coefficients.[41] The contribution of the symmetric OH stretching also added (0.5% or less). [c] Molecular absorption coefficient at band maximum, in dm^3 mol^{-1} cm^{-1}. fwhh, full width at half-height, in cm^{-1}. [d] The OH band in chloroform at 3531.4 cm^{-1} is asymmetric, and the two bands were obtained by fitting to two Lorentzians. [e] Sum of the intensities of the two modes of A and B symmetry since the difference in their frequencies is negligible. [f] The OH stretching participating in intermolecular H-bond. The band in THF was fitted to the Gaussian shape and the band in AN to the Lorentzian shape. [g] Calculated for non-H-bonded *ct*-BINOL (in italics).

vacuo is 332 cm^{-1}). Since in 2-phenylphenol it is observed at the higher wavenumber of 386 cm^{-1},[16] this is an evidence of the intramolecular hydrogen bond in the 2-phenylphenol. BINOL and other similar systems all have the νOH between 3600 and 3500 cm^{-1}, and the τCO is expected in the region 450−300 cm^{-1}. The calculated wavenumbers for the *cc*-isomer in CH_2Cl_2 are 440 (A) and 418 (B) cm^{-1} (Table 5), and for the *tt*-isomer in CH_2Cl_2 at 342 (A) and 333 (B) cm^{-1} (Table S3, Supporting Information). Furthermore, the absorption τCO should always be uniquely broad and thus easily distinguished from other fundamental absorptions. However, this is not observed in BINOL spectra. In the non-H-bonding solvents, all the bands in the 450−300 cm^{-1} region have their counterparts in the solid phase spectrum and are superimposed on a very broad absorption centered at ≈ 440 cm^{-1}. Its intensity rises in the order CCl_4, $CHCl_3$, and CH_2Cl_2. No such absorption is found for the H-bonding solvents, while at the same time, this is the only difference between the H- and non-H-bonding solution spectra. The modes of the *cc*-isomer in vacuo dominantly having the character of the torsional motion τCC′ are at 499.5 (A), 486.8 (A), and 447.7 (B) cm^{-1}; the same modes of the *ct*-isomer are at 437.7, 337.6, and 332.1 cm^{-1} and at 342.4 (A), 333.4 (B), and 332.3 (A) cm^{-1} for the *tt*-isomer. Thus, the torsional mode is shifted by ≈ 160 cm^{-1} to lower wavenumbers, and this shift is related to the free energy difference of 5.95 kcal/mol (Table 2) between the *cc*- and *tt*-conformers. In agreement with the decrease of the OH stretching frequency, the C1C1′ torsional modes are predicted at lower wavenumbers in solutions (Tables S1 (Supporting Information) and 5).

In order to correctly calculate a relative solvent induced wavenumber shift, δ, defined as

$$\delta = \frac{\tilde{\nu}_{solution} - \tilde{\nu}_{gas}}{\tilde{\nu}_{gas}}$$

or

$$\delta = \frac{\tilde{\nu}_{solvated} - \tilde{\nu}_{free}}{\tilde{\nu}_{free}}$$

the normal modes having the same nature should be compared. This is only possible if the intensity pattern between the gas phase and solution remains similar and the shifts themselves are small, say up to 1−3%. The corresponding potential energy distributions should also be calculated. Although the spectral changes from low (CCl_4, $\varepsilon = 2.23$) to medium dielectric medium (CH_2Cl_2, $\varepsilon = 8.93$) are expected to be much greater than from the medium to high dielectric medium (CH_3CN, $\varepsilon = 36.64$), all δ values, except those of the OH stretchings, are rearly

slightly above 1%. The largest shift of even 30% is predicted for the lowest mode that is actually pure internaphthyl torsion, i.e., small amplitude internal rotation of BINOL, but this could not have been observed. The observed relative wavenumber shift of the νOH gas band at 3562 cm^{-1} in dichloromethane is −0.9%, while the calculated one for *cc* is −0.5%. The shift of the weaker band at 3648 cm^{-1} in dichloromethane is −2.0%, and the calculated one for *tt* is −1.1%.

3.5. Spectra in Hydrogen Bond Accepting Solvents. We now consider solutions of BINOL in AN, THF, and DMF, i.e., in solvents that can form H-bonded complexes of various types with isomers of BINOL. The observed wavenumber shifts (relative to the gas phase) for modes other than those related to the OH groups in this group of solvents are again only up to 1% (Table S3, Supporting Information). Since even the *cc* isomer can be hydrogen bonded as a proton donor to a molecule belonging to any one of these H-bonding accepting solvents (this would be a strongly bent H-bond), the nature of the complexes in a given solvent cannot be unequivocally established. That this might happen in such solutions is also supported by the crystal structures of the BINOL inclusion compounds with acetone[5] and DMF.[6] At the same time, these solvents are all solvents of increased polarity, and the free energy differences between conformers get smaller because of the nonspecific interactions (Table 2). Since BINOL molecules are surrounded only by solvent molecules, various possible kinds of complexes are reduced to S···*cc*···S, S···*ct*···S, and S···*tt*···S, i.e., the complex of the type, for example, S···*cc* is considered almost improbable. There are a number of ways of how these complexes can be formed starting from *cc* isomers. Most probably, the transformation *cc*⇄*ct* takes place within the complex S···*cc*···S⇄S···*ct*···S and is rather fast. At the qualitative level, one would expect that the formation of an intermolecular H-bond will more than compensate for the energy difference between the two isomers. The trimers AN···*cc*···AN and AN···*tt*···AN that were already discussed in the gas phase were embedded in the polarizable continuum with $\varepsilon = 36.64$, i.e., acetonitrile, and the estimates for the free energies of solvation and formation were obtained in single-point calculations. The gas phase BSSE was used to correct the energies of trimers in AN. To avoid rather impractical geometry optimization (particularly in high permittivity continuum such as AN) of H-bonded complexes, the geometries were those of the gas phase except for the N···H distances. The analogous calculations of the methanol−acetonitrile complex have shown that the relative changes of the geometrical parameters relative to the monomer values were all up to 1% except for the N···H distance that suffered 5.7% shortening. Therefore, for the BINOL trimers the N···H distances were determined as the points of the lowest energies with all other geometry parameters frozen. The N···H distance in AN···*tt*···AN decreased from 2.0201 to 1.9419 Å, while in AN···*cc*···AN, it remained practically the same from 2.0090 to 2.0000 Å. Obviuosly, in the latter case steric effects prevent shorter N···H distances. As the free energies of trimer formation with all nonelectrostatic contributions included show (Table 4), only AN···*tt*···AN trimers should be present in solution, and this is confirmed by spectroscopic data also for the other two solvents, TMF and DMF. For example, the enthalpy of an intramolecular H-bond in 2-phenyl phenol measured in CC_4 is 1.45 kcal/mol,[14] and the enthalpy of an intermolecular H-bond between phenol and AN also in CCl_4 is 5.22 kcal/mol,[43] i.e., almost four times greater. Here the study of other, simpler alcohols with intramolecular H-bond in the same solvents might be of some help, and in this respect, a recently published kinetic study of the formation and dissociation of interintramolecular H-bond solvent (toluene)−solute (*ortho*-methoxyphenol) complexes presents highly relevant data.[44] The intramolecular H-bond of *ortho*-methoxyphenol is not broken, and yet, the solute−solvent complex occurs due to the intermolecular H-bond to the π-system of toluene.

In AN, an evidence for a weak band at around 3531 ± 6 cm^{-1} where a strong band in non-H-bonding solvents is found could not have been conclusively obtained probably because of the presence of much stronger solvent bands at 3621 and 3540 cm^{-1}. Intermolecular H-bonds are again observed as a broadband with a maximum at 3390 cm^{-1} and the full width at half-height of 200−250 cm^{-1}. Since the hydroxyl stretchings of phenol and 2-naphthol in AN are observed at 3400 cm^{-1} and 3385 cm^{-1}, respectively (Table S3, Supporting Information), most probably only the *tt*-isomers of BINOL are found in AN. In the OH stretching region of the THF solution with BINOL concentration between 0.005 and 0.1 mol dm^{-3}, there is a weak band at 3534 cm^{-1} that might be due to the uncomplexed *cc*-isomers. Hydrogen-bonded complexes of BINOL isomers are revealed by the strong and very broad band centered at 3295 cm^{-1}, which is 100 cm^{-1} lower than that in AN. It is very close to the corresponding band at 3297 cm^{-1} of phenol in THF, somewhat lower than the band at 3318 cm^{-1} of the *p*-fluorophenol−THF complex in CCl_4,[45] but higher than the 2-naphthol band in THF at 3276 cm^{-1} (Table S2, Supporting Information). Thus, again only the *tt*-isoners are present. The area under the 3295 cm^{-1} band linearly depends on BINOL concentration (Table 6). The pattern in DMF with a broad band centered at 3225 cm^{-1} is quite different in appearance. This broad characteristic is fully developed only at higher concentrations. At lower concentrations, the two overlapping bands at 3547 and 3494 cm^{-1} dominate. From the observed wavenumber shifts, the strongest hydrogen bond is thus formed between BINOL and DMF, which is expected because DMF has the largest β-value of the three H-bonding solvents. The H-bond between BINOL and DMF or THF is thus found lower than that for the phenol and DMF in CCl_4 that is observed at 3320 cm^{-1}[46] while for phenol and ketones such as acetone and acetophenone (also in CCl_4) at 3344 and 3367 cm^{-1},[40] respectively. Assuming that only *tt*-isomers are present in any of the H-bonding solvents, this difference must then be ascribed to nonspecific interactions with the highly polar polarizable continuum. Although the indications available also from other spectral regions show that the *tt* isomer is almost exclusively present in H-bonding solvents, the structure of the complexes nevertheless remains unresolved apart from the indications provided by the calculations (Table 4). This might be quite different from the crystal structures of BINOL inclusion compounds because an infinite H-bond network in crystal has quite different dynamics than an H-bonded complex in solution.

When comparing the calculated spectra of one isomer, say *cc*, in various solvents, the changes induced by nonspecific solute−solvent interactions are particulary obvious, as mentioned above, in the two regions, 1250 to 1050 cm^{-1} and 600 to 300 cm^{-1} (Figure 3). They are related to the redistribution of intensities. When comparing two isomers, say *cc* and *tt*, in the same solvent, the major differences are again predicted in the same regions. Since the wavenumbers of the OH in-plane bendings and CO stretching vibrations are rather close to each other, it is practically impossible to say what part of the intensity differences is due to the conformational change. For the *tt* isomer, the in-plane OH bending modes, βOH, occur together

with the CO stretching, νCO, between 1280 and 1150 cm^{-1} (Table S3, Supporting Information). The 1270 and 1179 cm^{-1} modes can be described as dominantly βOH vibration. In three others, at 1248, 1218, and 1204 cm^{-1}, the νCO contribution is the largest. Qualitatively, the same behavior is found in the recorded spectra. It is important that by observing the spectral region from 1250 to 1050 cm^{-1} the six solvents can be grouped the same way as according to their β-values.

There are differences between the spectra in non-H- and H-bonding solvents in other regions as well. The observed doublet centered around 1600 cm^{-1} with the bands of roughly equal intensity should thus be in favor of *cc*- and *ct*-isomers, even in more polar solvents. In the region 1250−1100 cm^{-1}, the significant differences between the spectra are found. The doublet at around 1600 cm^{-1} reverses its intensities (the lower band becomes weaker), and according to calculations, this is to be expected for the *tt*-isomer. However, it is interesting that the region from 600 to 300 cm^{-1} in CCl_4, $CHCl_3$, THF, and AN exhibits the same number of bands with practically unchanged relative intensities. However, while the other neighboring bands of the 467 cm^{-1} band in crystal are also found in solutions, this one is missing and seems to be replaced by the very broad and weak feature centered at $\sim$ 430 cm^{-1} in non-H-bonding solvents. In the H-bonding solvents (AN), this broad feature is shifted toward higher wavenumbers with the maximum at around 600 cm^{-1}. This might be explained by the formation of intermolecular H-bonds with solvent molecules because the 467 cm^{-1} band in crystal can be assigned to the pure CO torsion calculated at 448 cm^{-1} (Table S1, Supporting Information). Although the OH oscillators in the crystal are in two different bonding situations (one of them is bifurcated donor), there is no large difference in the corresponding frequencies, and therefore only one broadband is observed. According to calculations there are other normal modes in this region partaking of the nature of the hydroxyl group vibrations. The mode of the *cc* isomer in CH_2Cl_2 calculated at 494.3 cm^{-1} is dominantly in-plane bending βCO. It is therefore contrary to expectations to find that the observed spectra of BINOL solutions in H-bond accepting solvents are so similar to those in H-bond nonaccepting solvents. This could be considered as a strong indication of unchanged isomer preference on going from the gas phase to solution were it not for the observed changes in the OH stretching region. Thus, the hydroxyl hydrogens of BINOL participating in either intra- or intermolecular H-bonds do not substantially influence majority of the binaphthyl skeleton vibrations.

4. Conclusions

We have used literature IR (gas phase) and Raman (solid) spectra and have measured mid-IR spectra of BINOL and some structurally related compounds (phenol and 2-naphthol) in a series of organic solvents of increasing permittivity and ability to form hydrogen bonds. The spectra were analyzed and assigned by means of DFT reaction field calculations (the integral equation formalism[47] of the polarizable continuum model) of the three stable BINOL OH isomers. The vibrational frequencies (uniformly scaled by 0.9648, a factor based on the empirical assignment for phenol) and IR and Raman intensities calculated at the B3LYP/6−31+G(d) level of theory moderately agree with the experiment. In the regions of the OH vibrations, the agreement is quantitative neither for the gas phase nor for the non-H-bonding solvents. Besides the OH stretching region, the only other region where the notably changed intensity distribution was observed is the 1250−1100 cm^{-1} region. The strongest gas IR band at 1190 cm^{-1} is replaced by the strongest crystal IR band at 1176 cm^{-1}. In non-H-bonding solvents, this band is shifted to 1183 cm^{-1}. In all cases, it is attributed to the in-plane OH bending, βOH, mixed with the CO stretching, νCO. The 1183 cm^{-1} band remains strong, but the strongest is now at 1144 cm^{-1} that should be assigned to the aromatic in-plane CH bendings. However, the strongest Raman band in crystal at 1381 cm^{-1} is due to the CC stretchings of the central parts of the naphthyl moieities.

Comparison of the observed vibrational spectra with those calculated using the cavity built from overlapping spheres[48] suggests that a substantial part of the observed spectral changes can be attributed to the nonspecific part of molecular interactions. The *cc* isomer remains the most stable in solution with the energy difference between the isomers getting smaller with increasing solvent permittivity. The other two, *ct* and *tt* isomers, could thus be equally probable or even prevailing only in an H-bonding solvent because of the intermolecular H-bonds giving the complex that is lower in energy than the interintramolecular H-bonded complex. The absence of the weak band at 3590 ± 15 cm^{-1} in such a solvent assigned to the so-called free (not hydrogen bonded to another molecule) OH groups means that all BINOL molecules are hydrogen bonded. The question remains about the nature of the solute−solvent complex in this case since both types of complexes, S···*cc*···S and S···*tt*···S, are possible depending on the relative sizes of the various contributions to the enthalpy of complex formation. The latter seems substantially more probable as shown by the calculations in the case of acetonitrile and by comparison with similar systems (e.g., phenol and 2-naphthol) having OH groups attached to an aromatic group but lacking an intramolecular H-bond.

Because of the sizes of BINOL and solvent molecules, we have limited ourselves to the calculation of solvation effects without considering with all necessary details the formation of intermolecular H-bonds. However, the size of the system actually need not be a decisive factor in an attempt to include the specific interactions. More serious is the problem of positioning the solvent molecules and their number around the solute[49] because it immediately leads to the consideration of fluctuations, finite residence time of the coordinated solvent molecules, and so forth, which is beyond the scope of the present study.

Acknowledgment. This work was supported by the Ministry of Science, Education and Sport of the Republic of Croatia (Project No. 0982904-2927).

Supporting Information Available: Table S1 with the observed Raman (solid) and IR (gas and solid) wave numbers of BINOL and the scaled calculated wave numbers of the *cc*-isomer, Table S2 containing the observed wave numbers of the OH stretching vibrations in some related O−H···π systems and aryl-OH systems without the intramolecular hydrogen bond, and Table S3 with the observed wave numbers of BINOL in H-bond accepting solvents (acetonitrile, tetrahydrofuran, and *N*,*N*′-dimethylformamide) and the calculated wave numbers of the *tt*-isomer within the PCM for $\varepsilon = 8.93$ (dichloromethane). This material is available free of charge via the Internet at http://pubs.acs.org.

References and Notes

(1) Chen, Y.; Yekta, S.; Yudin, A. K. *Chem. Rev.* **2003**, *103*, 3155.
(2) Sahnoun, R.; Koseki, S.; Fujimura, Y. *J. Mol. Struct.* **2005**, *735/736*, 315.

(3) Meca, L.; Reha, D.; Havlas, Z. *J. Org. Chem.* **2003**, *68*, 5677.
(4) Mori, K.; Masada, Y.; Kashino, S. *Acta Crystallogr., Sect. C* **1993**, *49*, 1224.
(5) Nassimbeni, L. R.; Su, H. *New J. Chem.* **2002**, *26*, 989.
(6) Hirano, S.; Yoshizawa, K.; Toyota, S.; Toda, F.; Urbanczyk-Lipkowska, Z. *Mendeleev Commun.* **2003**, 141.
(7) Nakao, K.; Kiogoku, Y.; Sugeta, H. *Faraday Discuss.* **1994**, *99*, 77.
(8) Setnička, V.; Urbanova, M.; Bour, P.; Kral, V.; Volka, K. *J. Phys. Chem A* **2001**, *105*, 8931.
(9) Nogueira, H. I. S.; Quintal, S. M. O. *Spectrochim. Acta, Part A* **2000**, *56*, 959.
(10) Li, Z.-Y.; Chen, D.-M.; He, T.-J.; Liu, F.-C. *J. Phys. Chem. A* **2007**, *111*, 4767.
(11) Beckering, W. *J. Chem. Phys.* **1961**, *65*, 206.
(12) Baitinger, W. F.; Schleyer, P.; von, R.; Mislow, K. *J. Am. Chem. Soc.* **1965**, *87*, 3168.
(13) Baker, A. W.; Shulgin, A. T. *J. Am. Chem. Soc.* **1958**, *80*, 5358.
(14) Oki, M.; Iwamura, H. *Bull. Chem. Soc. Jpn.* **1960**, *33*, 717.
(15) Schleyer, P.; von, R.; Trifan, D. S.; Bacskai, R. *J. Am. Chem. Soc.* **1958**, *80*, 6691.
(16) Carlson, G. L.; Fateley, W. G. *J. Phys. Chem.* **1973**, *77*, 1157.
(17) Visser, T.; van der Maas, J. H. *Spectrochim. Acta, Part A* **1984**, *40*, 959.
(18) NIST/EPA Gas-Phase Infrared Database, http://webbook.nist.gov/chemistry.
(19) Baker, A. W.; Shulgin, A. T. *Spectrochim. Acta* **1963**, *19*, 1611.
(20) Kamlet, M. J.; Taft, R. W. *J. Org. Chem.* **1982**, *47*, 1734.
(21) Kamlet, M. J.; Abboud, J.-L. M.; Abraham, M. H.; Taft, R. W. *J. Org. Chem.* **1983**, *48*, 2877.
(22) Marcus, Y. *Chem. Soc. Rev.* **1993**, 409.
(23) Tomasi, J.; Mennucci, B.; Cammi, R. *Chem. Rev.* **2005**, *105*, 2999.
(24) Cammi, R.; Cappelli, C.; Corni, S.; Tomasi, J. *J. Phys. Chem A* **2000**, *104*, 9874.
(25) Furniss B. S; Hannaford A. J.; Smith P. W. G.; Tatchell A. R. *Vogel's Textbook of Practical Organic Chemistry*, 5th ed.; Longman: London, 1989.
(26) Bertie, J. E.; Dala Keefe, C.; Jones, R. N. *Tables of Intensities for the Calibration of Infrared Spectroscopic Measurements in the Liquid Phase*; IUPAC Chemical Data Series No. 40, Blackwell Science: Oxford, 1995.
(27) http://amiga.chemie.uni-konstanz.de/menges/spekwin/index.html.
(28) Frisch, M. J.; Trucks, G. W.; Schlegel, H. B.; Scuseria, G. E.; Robb, M. A.; Cheeseman, J. R.; Montgomery, J. A., Jr.; Vreven, T.; Kudin, K. N.; Burant, J. C.; Millam, J. M.; Iyengar, S. S.; Tomasi, J.; Barone, V.; Mennucci, B.; Cossi, M.; Scalmani, G.; Rega, N.; Petersson, G. A.; Nakatsuji, H.; Hada, M.; Ehara, M.; Toyota, K.; Fukuda, R.; Hasegawa, J.; Ishida, M.; Nakajima, T.; Honda, Y.; Kitao, O.; Nakai, H.; Klene, M.; Li, X.; Knox, J. E.; Hratchian, H. P.; Cross, J. B.; Bakken, V.; Adamo, C.; Jaramillo, J.; Gomperts, R.; Stratmann, R. E.; Yazyev, O.; Austin, A. J.; Cammi, R.; Pomelli, C.; Ochterski, J. W.; Ayala, P. Y.; Morokuma, K.; Voth, G. A.; Salvador, P.; Dannenberg, J. J.; Zakrzewski, V. G.; Dapprich, S.; Daniels, A. D.; Strain, M. C.; Farkas, O.; Malick, D. K.; Rabuck, A. D.; Raghavachari, K.; Foresman, J. B.; Ortiz, J. V.; Cui, Q.; Baboul, A. G.; Clifford, S.; Cioslowski, J.; Stefanov, B. B.; Liu, G.; Liashenko, A.; Piskorz, P.; Komaromi, I.; Martin, R. L.; Fox, D. J.; Keith, T.; Al-Laham, M. A.; Peng, C. Y.; Nanayakkara, A.; Challacombe, M.; Gill, P. M. W.; Johnson, B.; Chen, W.; Wong, M. W.; Gonzalez, C.; Pople, J. A. *Gaussian 03*, revision D.02; Gaussian, Inc.: Wallingford CT, 2004.
(29) Becke, A. D. *J. Chem. Phys.* **1993**, *98*, 5648.
(30) Lee, C.; Yang, W.; Parr, R. G. *Phys. Rev. B* **1988**, *37*, 785.
(31) Ditchfield, R.; Hehre, W. J.; Pople, J. A. *J. Chem. Phys.* **1971**, *54*, 724.
(32) Koch,W.; Holthausen, M. C. *A Chemist's Guide to Density Functional Theory*; Wiley-VCH: New York,2001.
(33) Evans, J. C. *Spectrochim. Acta* **1960**, *16*, 1382.
(34) Biliškov, N.; Zimmermann, B.; Baranović, G. *J. Mol. Struct.* **2003**, *661/662*, 65.
(35) Bondi, A. *J. Phys. Chem.* **1964**, *68*, 441.
(36) Preat, J.; Loos, P.-F.; Assfeld, X.; Jacquemin, D.; Perpete, E. A. *Int. J. Quantum Chem.* **2006**, *107*, 574.
(37) Korth, H.-G.; de Heer, M. I.; Mulder, P. *J. Phys. Chem. A* **2006**, *106*, 8779.
(38) Hollas, J. M.; Husein, M. Z. B. *J. Mol. Spectrosc.* **1988**, *127*, 497.
(39) Fateley, W. G.; Carlson, G. L.; Bentley, F. F. *J. Phys. Chem.* **1975**, *79*, 199.
(40) Widom, J. M.; Philippe, R. J.; Hobbs, M. E. *J. Am. Chem. Soc.* **1957**, *79*, 1383.
(41) Cappelli, C.; Corni, S.; Cammi, R.; Mennucci, B.; Tomasi, J. *J. Chem. Phys.* **2000**, *113*, 11270.
(42) Nyquist, R. A. *Spectrochim. Acta* **1963**, *19*, 1655.
(43) Sousa Lopes, M. C.; Thompson, H. W. *Spectrochim. Acta, Part A* **1968**, *24*, 1367.
(44) Zheng, J.; Kwak, K.; Chen, X.; Asbury, J. B.; Fayer, M. D. *J. Am. Chem. Soc.* **2006**, *128*, 2977.
(45) Arnett, E. M.; Mitchell, J. E.; Murty, T. S. S. R.; Gorrie, T. M.; Schleyer, P. V. R. *J. Am. Chem. Soc.* **1970**, *92*, 2365.
(46) Gramstad, T.; Funglevik, W. J. *Acta Chem. Scand.* **1962**, *16*, 1369.
(47) Cances, M. T.; Mennucci, B.; Tomasi, J. *J. Chem. Phys.* **1997**, *107*, 3032.
(48) Vibrational calculations using the the reaction field with the spherical cavity predicted practically no other effect besides an overall increase in intensity, which is in a way in agreement with the experiment. However, the calculated enthalpy differences are much too large to account for the occurence of other BINOL isomers.
(49) da Silva, C. O.; Mennucci, B.; Vreven, T. *J. Phys. Chem. A* **2003**, *107*, 6630.

JP801868X